EPJ manuscript No.
(will be inserted by the editor)

Two-colour Quantum Entanglement in a Singly Resonant Optical Parametric Oscillator Approaching Threshold

Domenico Cuozzo, John Jeffers, and Gian-Luca Oppo

ICS, SUPA and Department of Physics, University of Strathclyde, Glasgow G4 0NG, Scotland, U.K.

February 8, 2012

Abstract. Following the analytical work of Ref. [1], a numerical analysis of squeezing and quantum entanglement in a continuous wave singly-resonant optical parametric oscillator approaching threshold is provided. The singly resonant case is mainly relevant to largely non-degenerate signal and idler modes (two-colour output). As the threshold of oscillation is approached the numerical spectra of the intensity difference confirm squeezing of quantum fluctuations and a progressive line-narrowing in the linear case. In the nonlinear case entanglement is confirmed although progressively reduced when approaching threshold with the squeezing spectra still displaying a narrowing of the spectral line. Modification of quantum entanglement approaching threshold is also evaluated via the condition of state inseparability.

PACS. 42.50.Lc – 42.50.Dv – 42.65.Yj

1 Introduction

Continuous variable squeezed states of light, where the noise in one quadrature of the fields is reduced below the vacuum level, have found several applications in quantum information [2]. For example, squeezed states are used to generate continuous variable entanglement and achieve high fidelity in quantum teleportation protocols [2]. In order to be squeezed, quantum fluctuations of the electromagnetic field require nonlinear optical effects such as parametric down-conversion or four-wave mixing [3]. Here we focus on intra-cavity parametric down-conversion of a pump photon at frequency ω_p into a photon at frequency ω_s, the signal, and another at ω_i, the idler, inside a nonlinear crystal with a second order nonlinear susceptibility $\chi^{(2)}$ [3]. The so-called "non-degenerate case" corresponds to separate signal and idler frequencies. Parametric down-conversion in an optical cavity is known as an Optical Parametric Oscillator (OPO) where the oscillation build-up inside the cavity increases noise reduction by considerably extending the interaction time. Several theoretical and experimental investigations of squeezing in non-degenerate OPOs focused on the doubly (or even triply) resonant configurations where both the signal and idler fields are resonated [5,6,4]. Although the singly-resonant cavity is, in principle, a simpler configuration to realise experimentally, theoretical investigations of quantum entanglement in a singly-resonant OPO (SROPO) have been done only very recently [1]. Here it was shown that both intensity and quadrature squeezing are present in the SROPO below threshold and that the maximum noise reduction below the standard quantum limit is the same at the signal and idler frequencies in a similar way to the doubly-resonant case. As the threshold of oscillation is approached, however, the intensity-difference and quadrature spectra display a progressive line-narrowing which is absent in the balanced doubly-resonant case. One of the reasons for the lack of squeezing experiments in SROPOs is that they operate with strongly non-degenerate frequencies (two-colours). Since the observation of non-classical correlations in the strongly non-degenerate regime of parametric down-conversion [18], however, investigations of quantum entanglement in SROPO have gained relevance because of possible optimisation of coherent sources with fluctuations below the shot-noise level. Moreover, SROPOs have clear technical advantages over doubly-resonant configurations such as continuous temperature tuning and suppression of mode-hopping. It is the aim of this work to compare the analytic results of [1] for the squeezing and entanglement properties of SROPOs with a numerical analysis of both the linear and nonlinear regimes approaching threshold. In the nonlinear case we observe a progressive reduction of squeezing and quantum entanglement while the novel feature of SROPO of narrowing of the spectral line survives although it is reduced while approaching the threshold of oscillation.

Correspondence to: domenico.cuozzo@strath.ac.uk and/or g.l.oppo@strath.ac.uk

2 Quantum Langevin equation

We consider parametric down-conversion in a monolithic cavity resonant to the signal field only and pumped with a monochromatic beam at frequency ω_p (see Fig. 1).

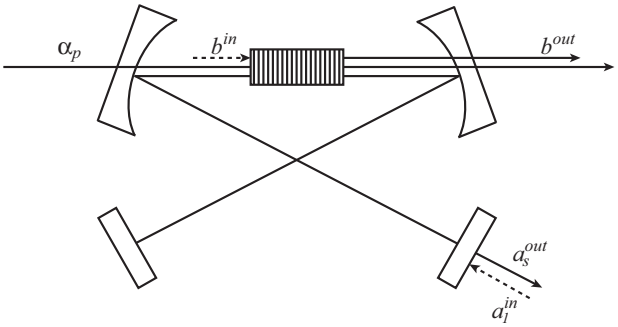

Fig. 1. The singly-resonant OPO cavity scheme. α_p is the input pump amplitude, a_1^{in} and b^{in} are the input signal and idler fields, a_s^{out} and b^{out} are the output signal and idler fields.

By assuming perfect collinear phase matching and considering energy conservation, one has [3]:

$$\boldsymbol{k}_p = \boldsymbol{k}_s + \boldsymbol{k}_i, \tag{1}$$
$$\omega_p = \omega_s + \omega_i, \tag{2}$$

where $\boldsymbol{k}_p$, $\boldsymbol{k}_s$ and $\boldsymbol{k}_i$ are the wavevectors of the pump, the signal and the idler fields respectively. In the case of perfect phase matching the frequencies of the signal and idler fields depend only on the frequency of the pump and the orientation of the crystal with respect to the direction of the pump beam. The quantum mechanical Hamiltonian for the system in the rotating-wave approximation is:

$$H = H_{sys} + H_{bath,1} + H_{bath,2} + H_{int,1} + H_{int,2} + H_{int,3}. \tag{3}$$

where H_{sys} is the sum of the free energies for the single signal mode, a_s, a continuum of idler modes, $b(\omega)$, and a continuum of pump modes, $a_p(\omega)$, treated here using the approach of [10]; $H_{bath,1}$ is the free energy of bosonic heat bath modes, $c_1(\omega)$, providing a description of the field external to the cavity and coupled to the signal because of non-perfect reflection of the mirrors [11]; $H_{int,1}$ in the Hamiltonian (3) represents the interaction of the signal mode with this heat bath, describing the damping of the signal mode caused by the non-zero transmittivity of the cavity; $H_{bath,2}$ is the free energy of different bosonic heat bath modes, $c_2(\omega)$, while the term $H_{int,2}$ is the interaction between the signal field and these modes, describing the damping of the signal mode associated with other loss mechanisms like other mirror transmissions or crystal absorptions and diffraction; the term $H_{int,3}$ is the interaction between the signal, idler and pump modes, treated here as a continuum of modes since the pump is not resonated in the cavity, describing the process of parametric down-conversion inside the nonlinear crystal [3]. In the rotating wave approximation, all these terms have explicit forms given by:

$$H_{sys} = \hbar\omega_s a_s^\dagger a_s + \hbar\int_{-\infty}^{\infty} d\omega\, \omega b^\dagger(\omega) b(\omega), \tag{4}$$
$$H_{bath,1} = \hbar\int_{-\infty}^{\infty} d\omega\, \omega c_1^\dagger(\omega) c_1(\omega), \tag{5}$$
$$H_{bath,2} = \hbar\int_{-\infty}^{\infty} d\omega\, \omega c_2^\dagger(\omega) c_2(\omega), \tag{6}$$
$$H_{int,1} = i\hbar\int_{-\infty}^{\infty} d\omega\, \kappa_1 \left[c_1(\omega) a_s^\dagger - c_1^\dagger(\omega) a_s\right], \tag{7}$$
$$H_{int,2} = i\hbar\int_{-\infty}^{\infty} d\omega\, \kappa_2 \left[c_2(\omega) a_s^\dagger - c_2^\dagger(\omega) a_s\right], \tag{8}$$
$$H_{int,3} = i\hbar\int_{-\infty}^{\infty} d\omega \int_{-\infty}^{\infty} d\omega'\, \kappa_3 \left[b^\dagger(\omega) a_s^\dagger a_p(\omega') b(\omega) a_s a_p^\dagger(\omega')\right]. \tag{9}$$

The coupling constants κ_1, κ_2, and κ_3 are considered to be independent of the frequency ω according to the Markov approximation. We also consider the following commutation relations for the modes:

$$[a_s, a_s^\dagger] = 1, \tag{10}$$
$$[a_p(\omega), a_p^\dagger(\omega')] = \delta(\omega - \omega') \tag{11}$$
$$[c_i(\omega), c_i^\dagger(\omega')] = \delta(\omega - \omega'), \tag{12}$$
$$[b(\omega), b^\dagger(\omega')] = \delta(\omega - \omega'), \tag{13}$$

where $i = 1, 2$ while all the other commutators are identically zero. For the non-resonant idler field we use the theory of Collett and Levien [12] who showed that systems described by a continuum of mode operators $\bar{b}(\omega)$ and possessing an isolated mode of particular interest, can be redescribed in terms of an orthonormal set formed by this one mode and a new continuum $b(\omega)$. From (3-9) one can derive a Heisenberg-Langevin equation of motion for the evolution of the signal field below the threshold of oscillation in the interaction picture:

$$\frac{d}{dt} a_s = \gamma\varepsilon^2 \frac{a_s}{\left[1 + g a_s^\dagger a_s\right]^2} - \gamma a_s - \sqrt{2\gamma}\varepsilon b^{\dagger in} + \sqrt{2\gamma_1} a_1^{in} + \sqrt{2\gamma_2} a_2^{in}. \tag{14}$$

where $g = k_3^2\pi^2$, b^{in} is the idler field noise, $\gamma_1 = \kappa_1^2\pi$ is the signal cavity damping rate and a_1^{in} the input vacuum modes entering the cavity from the environment. The term $\gamma_2 = \kappa_2^2\pi$ is the intracavity loss rate, mainly due to absorption by the crystal, while a_2^{in} is the quantum noise associated with this loss and defined in the usual way [10]. We also consider $\gamma = \gamma_1 + \gamma_2$ as the total damping rate and ε to parametrize the classical external pump value α_p, below threshold $\alpha_p = \varepsilon\alpha_{th}$, where $\alpha_{th} = \sqrt{\gamma/(2\pi^2 k_3^2)}$ so that $0 < \varepsilon < 1$. Note that there is no detuning in Eq. (14) since any change in the cavity length is compensated by a change in the signal (and idler) frequency, a property typical of SROPO configurations. Finally it is useful

to introduce the number of photons at threshold given by $n_{th} = \alpha_{th}^2 = \gamma/2g$ that characterises the pump intensity necessary to achieve signal generation in the optical cavity. In addition to the Langevin equation (14) there are boundary conditions, known as input-output relations:

$$a_s^{out} = \sqrt{2\gamma_1}a_s - a_1^{in}, \tag{15}$$
$$b^{out} = \epsilon\sqrt{2\gamma}a_s^{\dagger} - b^{in}. \tag{16}$$

Note that the input-output relation of the signal field is written at the cavity mirror of the SROPO while that of the idler field makes explicit the propagation of the idler fluctuations through the crystal (see Fig. 1). The input fields satisfy the following commutation relations:

$$[a_i^{in}(t), a_i^{\dagger in}(t^{'})] = \delta(t-t'), \tag{17}$$
$$[b^{in}(t), b^{\dagger in}(t^{'})] = \delta(t-t') \tag{18}$$

where $i = 1, 2$. Similar relations hold for the output fields while all the other commutators are vanishing.

For completeness we present the explicit expressions for the input and output fields, following the usual definition of [17]:

$$\begin{aligned} a_i^{in}(t) &= -\frac{1}{\sqrt{2\pi}}\int_{-\infty}^{+\infty} d\omega\, e^{-\imath\omega(t-t_0)}c_i^0(\omega) \\ b^{in}(t) &= -\frac{1}{\sqrt{2\pi}}\int_{-\infty}^{+\infty} d\omega\, e^{-\imath\omega(t-t_0)}b^0(\omega) \\ a_i^{out}(t) &= \frac{1}{\sqrt{2\pi}}\int_{-\infty}^{+\infty} d\omega\, e^{-\imath\omega(t-t_1)}c_i^1(\omega) \\ b^{out}(t) &= \frac{1}{\sqrt{2\pi}}\int_{-\infty}^{+\infty} d\omega\, e^{-\imath\omega(t-t_1)}b^1(\omega) \end{aligned} \tag{19}$$

where $i = 1, 2$, $t_0 < t$ and $c_i^0(\omega)$ and $b^0(\omega)$ are the values of $c_i(\omega)$ and $b(\omega)$ at $t = t_0$, respectively, while $t_1 > t$ and $c_i^1(\omega)$ and $b^1(\omega)$ are the values of $c_i(\omega)$ and $b(\omega)$ at $t = t_1$, respectively. We consider the input noise to be a Gaussian distributed white noise and the heat bath to be at zero temperature. In this basis the correlation functions for the input fields are:

$$\left\langle a_i^{in}(t)a_i^{\dagger in}(t^{'})\right\rangle = \left\langle b^{in}(t)b^{\dagger in}(t^{'})\right\rangle = \delta(\tau), \tag{20}$$

where $i = 1, 2$ and where we have defined $\tau = t - t'$.

3 Direct detection of intensity fluctuations

3.1 The linear case

Direct detection of intensity fluctuations of the signal and idler fields is the simplest type of quantum measurement one can perform in a two-colour OPO. A reduction in the intensity-difference fluctuations below the shot noise level in doubly-resonant OPOs above the threshold of oscillation was calculated by Reynaud et al. [13] and Lane, Reid and Walls [14] and demonstrated by Heidmann et al. [15] for a Type II non-degenerate OPO. The study of signal-idler intensity fluctuations in a SROPO below the threshold of oscillation was treated analytically in [1]. In this type of measurement the signal and idler fields hit two different photodetectors and then the resulting difference intensity fluctuations are studied with a power spectrum analyzer. The measurable output is related to the Fourier transform of the intensity-difference correlation function:

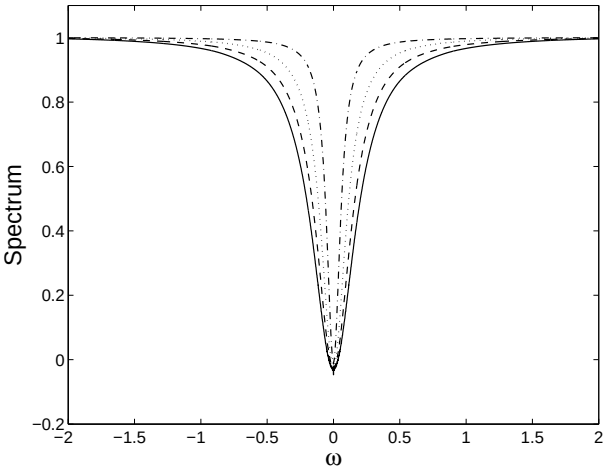

Fig. 2. Intensity difference correlation spectrum of (21) plotted for a range of input powers. Curves correspond to $\varepsilon = 0.6$ (solid line), $\varepsilon = 0.7$ (dashed line), $\varepsilon = 0.8$ (dotted line), $\varepsilon = 0.9$ (dash-dotted line) and $g = 0$ (linear case).

$$\frac{S_D[\omega]}{S_0} = 1 + \frac{1}{S_0}\int_{-\infty}^{+\infty} d\tau \left\langle : I_D^{out}(0), I_D^{out}(\tau) : \right\rangle e^{i\omega\tau}, \tag{21}$$

where $I_D^{out}(t) = a_s^{\dagger out}(t)a_s^{out}(t) - b^{\dagger out}(t)b^{out}(t)$ is the output difference intensity operator for signal and idler fields, S_0 is the shot noise level given in this case by the sum of the intensities of signal and idler beams, $S_0 = I_s^{out} + I_I^{out}$, and colons denote normal ordering. Furthermore, for any operators A and B:

$$\langle A, B\rangle = \langle AB\rangle - \langle A\rangle\langle B\rangle. \tag{22}$$

In order to relate the theoretical approach to the numerical simulations we express the normally ordered correlation function and spectrum of Eq. (21) in terms of equivalent c-number quantities in the Wigner representation. To this end we use the following correspondence:

$$\begin{aligned} C = \left\langle a_s^{\dagger out}(t)a_s^{out}(t+\tau)\right\rangle &= \left\langle \alpha_s^{*out}(t)\alpha_s^{out}(t+\tau)\right\rangle \\ &- \frac{1}{2}\exp(-\gamma(1-\varepsilon^2)|\tau|) \end{aligned} \tag{23}$$

$$\left\langle : I_D^{out}(0), I_D^{out}(\tau) : \right\rangle = C^2\frac{\gamma(1-\varepsilon^2)(2-\varepsilon^{-2}-\varepsilon^2)}{\varepsilon^2}. \tag{24}$$

For simplicity we consider in this paper the case of $\gamma_2 = 0$, i.e. $\gamma = \gamma_1$ but the results can be easily generalised to the case that includes crystal absorption.

The spectrum (21) is shown in Fig. 2 for different values of the pump parameter ε and for the linear case corresponding to $g = 0$. A progressive narrowing of the spectrum when approaching threshold clearly confirms the analytic formula of [1]:

$$\frac{S_D[\Omega]}{S_0} = 1 - \frac{4}{4 + [\Omega/(1-\varepsilon^2)]^2} \,. \tag{25}$$

Curves corresponding to the analytical form (27) are not presented in Fig. 2 because they are not distinguishable from those obtained by the numerical integration of Eq. (14). The numerical analysis then confirms that the narrowing of the spectral line is a function of the pump parameter ε and that squeezing below the shot noise is indeed possible in the SROPO. It is worth noting that perfect suppression of noise below the shot noise level is achievable at resonance independently of the pump power in the SROPO.

3.2 The nonlinear case

The spectra (21) in the nonlinear case are shown in Fig. 3(a)-(b) for different values of the pump parameter, ε, and for $g = 0.001$ and $g = 0.01$, respectively. It is clear that when approaching the threshold of oscillation, the squeezing level decreases and vanishes exactly at threshold. This behaviour is not due to the narrowing of the spectral lines which is characteristic of the linear case (see Fig. 2 and Eq. (21)), but instead to the effect of the nonlinear term in Eq. (14).

In Fig. 4 we plot the spectrum of (21) for $\varepsilon = 0.9$ and for increasing values of g. We note that going from $g = 0.0$ to $g = 0.01$ decreases the squeezing value and at the same time produces a broadening of the spectral line.

The effect of the nonlinearity of Eq. (21) on the spectral minimum and spectral broadening of the intensity difference for different values of g is presented in Fig. 5(a)-(b), respectively. The deterioration of squeezing approaching threshold due to recombination and saturation in OPOs has been known for some time [16]. One spectral feature that is instead peculiar to the singly resonant case is that of the spectral line narrowing. Although the narrowing approaching threshold is reduced when the number of photons decreases, line narrowing is still present even when the saturating effects of the nonlinearity are considered. This means that in realistic configurations of the SROPO, squeezing, quantum entanglement and progressive narrowing of the spectral line should be measurable experimentally.

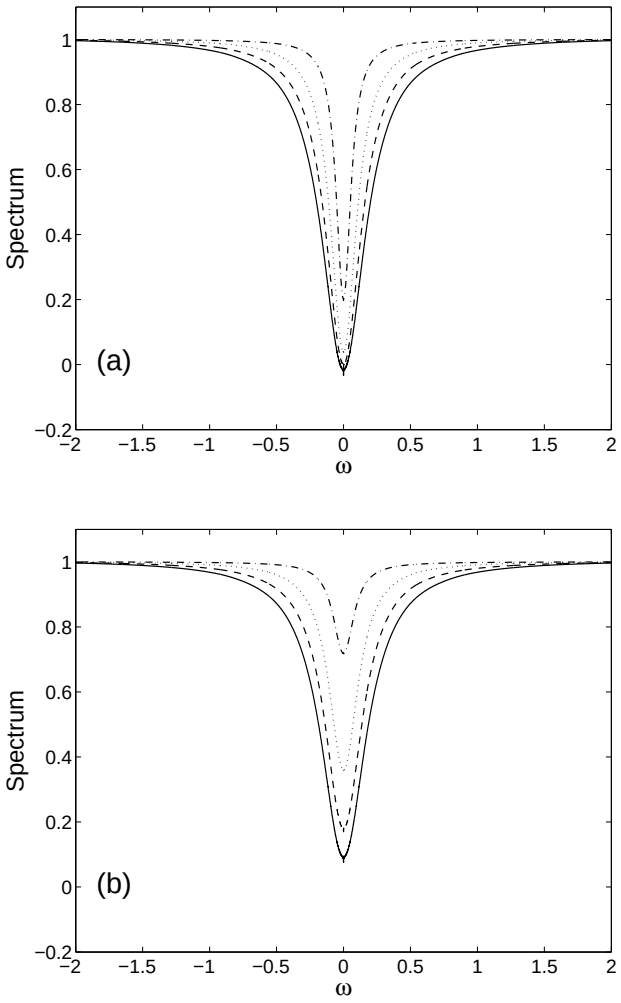

Fig. 3. Intensity-difference correlation spectrum of (21) plotted for a range of input powers. Curves correspond to $\varepsilon = 0.6$ (solid line), $\varepsilon = 0.7$ (dashed line), $\varepsilon = 0.8$ (dotted line), $\varepsilon = 0.9$ (dash-dotted line) and (a) $g = 0.001$ and (b) $g = 0.01$, respectively.

4 Quantum entanglement; the condition of state inseparability

In order to claim state inseparability and consequently entanglement for the signal-idler state we apply the separability criterion of Simon-Duan [17,18]. According to this criterion a sufficient condition for state inseparability written for the quadrature operators of the signal and idler beams

$$\begin{aligned} X^s_\theta(t) &= a_s(t)e^{i(\theta+\omega_s t)} + a^\dagger_s(t)e^{-i(\theta+\omega_s t)}, \\ X^i_\phi(t) &= b(t)e^{i(\phi+\omega_i t)} + b^\dagger(t)e^{-i(\phi+\omega_i t)}, \end{aligned} \tag{26}$$

where θ and ϕ are quadrature angles, is that the quantity:

$$S = \left\langle [X^s_\theta - X^i_\phi]^2 \right\rangle + \left\langle [X^s_{\theta+\pi/2} + X^i_{\phi+\pi/2}]^2 \right\rangle \tag{27}$$

is such that:

$$S < 2. \tag{28}$$

It is possible to connect the quantity S to the intracavity correlation function C introduced in (23):

$$S = 2\left[\left(4\gamma - \frac{2\gamma(1+\varepsilon^2)}{\varepsilon}\right)\mathcal{F}[C] + 1\right]. \tag{29}$$

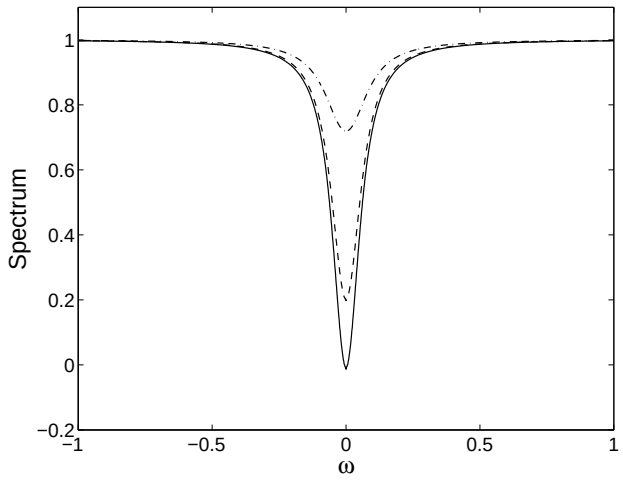

Fig. 4. Intensity-difference correlation spectrum of (21) plotted for $\varepsilon = 0.8$. Curves correspond to $g = 0$ (solid line), $g = 0.001$ (dashed line), and $g = 0.01$ (dash-dotted line).

where $\mathcal{F}[C]$ is the Fourier Transform of C and the expression must be evaluated at zero frequency. The quantity C can be directly evaluated from numerical simulations of the Langevin equations (14) in both linear ($g = 0$) and nonlinear regimes. These reasults can be compared with the analytical expression of S:

$$S = 2\left[\left(4 - \frac{2(1+\varepsilon^2)}{\varepsilon}\right)\frac{2\varepsilon^2}{(1-\varepsilon^2)^2} + 1\right] \qquad (30)$$

Fig. 6 shows a comparison of the Simon-Duan coefficient, S, for theory and numerical simulations in the linear regime, and two examples of the nonlinear case for $g = 0.001$ and $g = 0.01$. The evaluation of S critically depends on the tails of the correlation function, C, where the numerical simulations display large fluctuations. Although the value of S from the numerical simulations is systematically higher than the analytical result, it still reproduces the overall variation with the pump parameter and clearly shows that quantum entanglement is commonplace in SROPOs since S is well below the limit of 2. When the nonlinear term is included, entanglement is reduced but not entirely eliminated as shown in Fig. 6. We conclude that SROPOs can be excellent candidates for the generation of two-colour quantum entangled states over wide ranges of parameter values and different configurations of operation as anticipated in [1].

5 Conclusions

Squeezing and quantum entanglement in OPOs has been theoretically predicted and experimentally detected for a long time. The case of singly resonant OPOs, however, has been overlooked since preference has been given to frequency degenerate cases or cavity configurations where more than one field is resonated. We have recently described quantum squeezing and entanglement in SROPOs

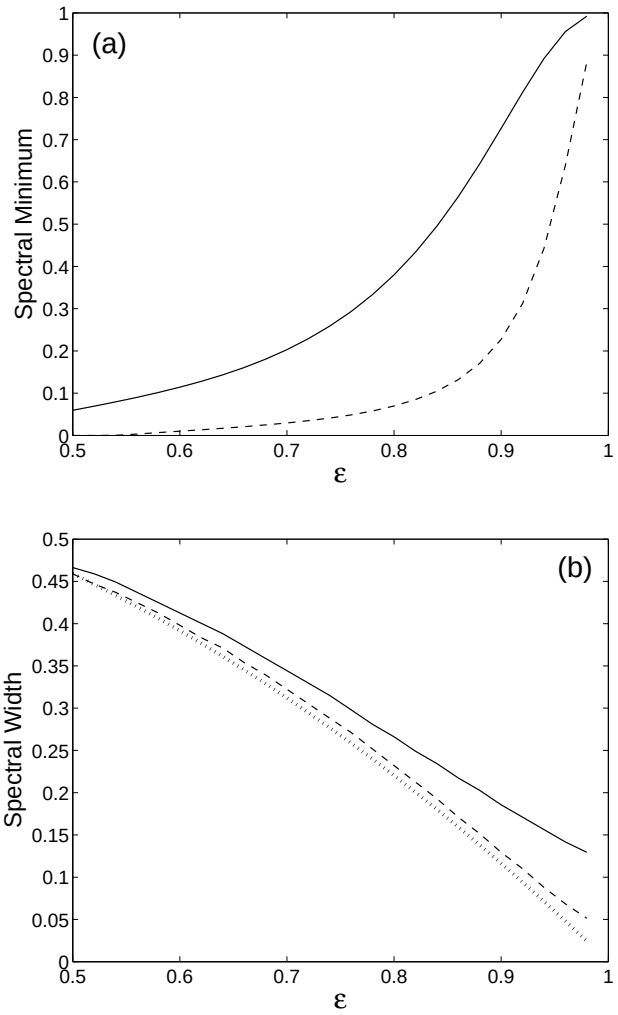

Fig. 5. (a) Minimum of the spectrum (21) of the intensity-difference correlation function versus the input power ε for $g = 0.01$ (solid line) and $g = 0.001$ (dashed line). (b) Full-width at half-minimum of the spectrum (21) of the intensity-difference correlation function versus the input power ε for $g = 0.01$ (solid line), $g = 0.001$ (dashed line) and the linear case for $g = 0$ (dotted line).

and found a feature that is not present in the doubly-resonant case: the spectrum of the intensity difference between the signal and idler fields progressively narrows when approaching threshold [1].

Here we have first verified that both squeezing and spectral line narrowing are present in numerical simulations of the Langevin equations describing quantum fluctuations in a SROPO below threshold. The numerical integration of these equations becomes necessary when exploring regimes where the linear approximation fails. As an example, we have investigated the role of the optical nonlinearity on the squeezing spectrum of the intensity difference and the conditions of state inseparability when approaching threshold of oscillation. The spectral minimum that remained at zero in the linear case for all values

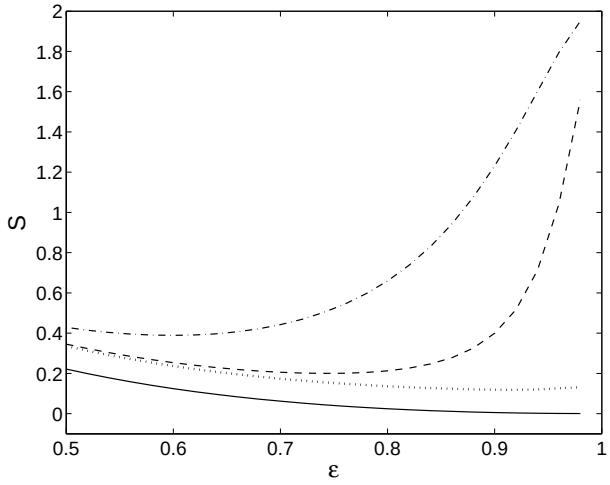

Fig. 6. The Simon-Duan state nonseparabilty coefficient S versus the pump parameter ε. Theory from Eq. (30) (solid line), numerical simulations for $g = 0.0$ (dotted line), $g = 0.001$ (dashed line) and $g = 0.01$ (dashed-dotted line).

of the input pump, gradually increases when approaching threshold in the nonlinear case. For small values of g, i.e. large photon numbers at threshold, reduction of quantum fluctuations below the shot noise is still visible close to threshold. The line narrowing of the squeezing spectrum is also reduced but still visible even in the nonlinear case. Finally, quantum entanglement via the state inseparability condition of Simon and Duan has been analysed in the SROPO model for both the linear and nonlinear regime. In the linear regime entanglement is predicted for wide ranges of the pump parameter below threhsold and well below the limit imposed by the state inseparability condition. In the nonlinear regime, entanglement is reduced close to threshold but the condition of state inseparability between the two colour signal and idler fields is still satisifed. The numerical methods developed here for the investigation of squeezing and quantum entanglement are then ready to be exported to the study of giant noise amplification in synchronously pumped SROPOs.

Acknowledgments

We acknowledge financial support from the EU commission through the IST network project HIDEAS (grant No. FP7-ICT-221906). We thank Alison Yao for help in the preparation of Fig. 1 and useful discussions.

References

1. D. Cuozzo and G.-L. Oppo, Phys. Rev. A **84**, 043810 (2011).
2. S. L. Braunstein, P. Van Loock, Reviews of Modern Physics **77**, 513 (2005).
3. L. Mandel and E. Wolf, Optical Coherence and Quantum Optics (Cambridge University Press, Cambridge, 1995).
4. C. Fabre, E. Giacobino, A. Heidmann and S. Reynaud, J. Phys. France **50** 1209 (1989).
5. C. Schori, J. L. Sorensen and E. S. Polzik, Phys. Rev. A **66**, 033802 (2002).
6. J. Laurat, T. Coudreau, G. Keller, N. Treps, and C. Fabre, Phys. Rev. A **71**, 022313 (2005).
7. C. W. Gardiner and P. Zoller, Quantum Noise, (Springer, Berlin, 2004).
8. D. F. Walls and Gerard J. Milburn, Quantum Optics, (Springer, Berlin, 2008).
9. I. N. Agafonov, M. V. Chekhova and G. Leuchs, Phys. Rev. A. **82**, 011801(R) (2010).
10. K. J. Blow, R. Loudon, S. J. D. Phoenix, and T. J. Shepherd Phys. Rev. A **42**, 4102 (1990).
11. M. J. Collett and C. W. Gardiner, Phys. Rev. A **30**, 1386 (1984).
12. M. J. Collett and R. B. Levien, Phys. Rev. A **43**, 5068 (1991).
13. S. Reynaud, C. Fabre and E. Giacobino, J. Opt. Soc. Am. B **4**, 1520 (1988).
14. A. S. Lane, M. D. Reid and D. F. Walls, Phys. Rev. A. **38**, 788 (1988).
15. A. Heidmann, R. J. Horowicz, S. Reynaud, E. Giacobino, C. Fabre and G. Camy, Phys. Rev. Lett. **59**, 2555 (1987).
16. E. G. Lariontsev and I. I. Zolotoverkh, J. Opt. B **4**, 15 (2002).
17. R. Simon, Phys. Rev. Lett. **84**, 2726 (2000).
18. L. M. Duan, G. Giedke, J. I. Cirac and P. Zoller, Phys. Rev. Lett. **84**, 2722 (2000).